

Concentration effect on anodizing aluminum oxide formation and its application in fabrication of fish-bone like nanochannels

Bin Huang¹, Yifu Guo¹, Yunlong Tian¹, Yanwei Wen¹, Bin Shan¹, Rong Chen^{2*}

¹State Key Laboratory of Material Processing and Die & Mould Technology, School of Materials Science and Engineering,

²State Key Laboratory of Digital Manufacturing Equipment and Technology, School of Mechanical Science and Engineering,

Huazhong University of Science and Technology, Wuhan 430074, Hubei, People's Republic of China

In this paper, we report a systematic study on the influence of oxalic acid concentration on the structural feature of anodic aluminum oxide including pore size, inter pore distance and growth rate. Our results show that the main effect of oxalic acid electrolyte is to enhance the growth rate, with little effect on pore size and inter pore distance distributions. High electrolyte concentration could also promote the branched growth of AAO during a voltage lowering process, which opens new avenue for the fabrication of new types of nanostructured channels. As an illustration, we demonstrate the formation of “fish-bone” like AAO nanochannels by optimizing the growth condition, and show its superior hydrophilicity which allows improved pore filtration for template synthesis.

Introduction

Anodic aluminum oxide (AAO) is widely used as template to fabricate one-dimensional nano material mainly due to its ordered hexagonal array of cylindrical nanochannels and controllable morphology (1). The growth of AAO film is affected by several anodizing parameters, including anodizing voltage, temperature, and types of electrolyte. Among them, anodizing voltage has been widely studied. It often gives a linear relationship with AAO pore size and inter pore distance distribution. Also the growth rate can be dramatically promoted with high anodizing voltage and temperature (2). Recently, studies on fabricating branched-channel AAO nanostructures are growing (3, 4). The three-dimensional structures have potential to widen AAO's application in nano technology such as chemical sensor, photonic device and filtration (5, 6). In addition, it provides a promising way to fabricate complex nanostructures (7, 8). To our best knowledge, there are only very few reports focused on studying the electrolyte concentration effects, nor optimizing concentration to achieve branched nano-channels.

In this paper, we present a detailed analysis and discussion on electrolyte concentration effect to AAO direct and branched nano-channels. It was found that the high electrolyte concentration can promote the growth rate without affecting the pore size and inter pore distance of AAO. Furthermore, the branched growth of AAO template will also be discussed in different experimental condition. By combining the anodizing

voltage and suitable electrolyte concentration, we show the formation of “fish-bone” like AAO nano-channels.

Experiment

AAO membranes were fabricated by a well-known two step anodizing method. High purity aluminum foils (99.999%) were cut into 20mm × 35mm × 0.3mm pieces, degreased in acetone for several minutes followed by DI water rinsing. The annealing process was then carried out under nitrogen purge at 500°C for 4 hours in order to enhance the grain size and release the mechanical stress. Subsequently, samples were electropolished at 18V for 5min in ethanol and perchloric acid mixture (1:5 volume ratio). To investigate the oxalic acid concentration effect, anodization was performed in different concentrations of oxalic acid (0.15M, 0.3M, 0.6M and 0.9M) with voltage ranging from 30V to 60V. To compare the morphology by different electrolytes, specimens were also fabricated in 0.3M sulfuric acid with voltage ranging from 15V to 30V. The anodizing temperature was kept at 20°C. To reduce the influences of chemical etch from electrolyte, the first anodization was last for 0.5h. Before second anodization, the aluminum foils were immersed in the mixture acid of 5wt% H₃PO₄ and 1.8wt% H₂CrO₄ at 60°C to remove surface oxidation layer. The samples' conductivity was checked to ensure the surface alumina was completely etched away. Then the second anodization was conducted at the same anodizing condition for another 0.5h.

To study the branched growth of AAO, anodization was conducted with different voltage-time curve. The current-time transient of anodizing was recorded by a programmable power source. A field emission scanning electron microscope (FE-SEM, JSM-7600) was employed to image the top views and cross-section images. Commercial available software ImageJ 1.46 was utilized to obtain statistical values on the pore size and inter pore distance distributions.

Results and Discussions

Types of electrolyte: a brief comparison on AAOs form in sulfuric acid and oxalic acid

Parameters affected morphology of AAO have been widely reported (9, 10). Major parameters include anodizing voltage, electrolyte type, etch time and temperature. Here we compared two kinds of electrolytes, sulfuric acid and oxalic acid, in a wide range of anodizing voltages. Figure 1 compares AAO samples formed in sulfuric acid (Figure 1(a)) and oxalic acid (Figure 1(b)). Both of them show ordered-hexagonal pore arrangement. The ordered arrangement can maintain a wide voltage range in oxalic acid (30V-50V) than those in sulfuric acid (20V-25V). Since voltage is the most important parameter to control pore size, pores are smaller in sulfuric acid (14.5nm-22.8nm) than those in oxalic acid (26.3nm-41.5nm).

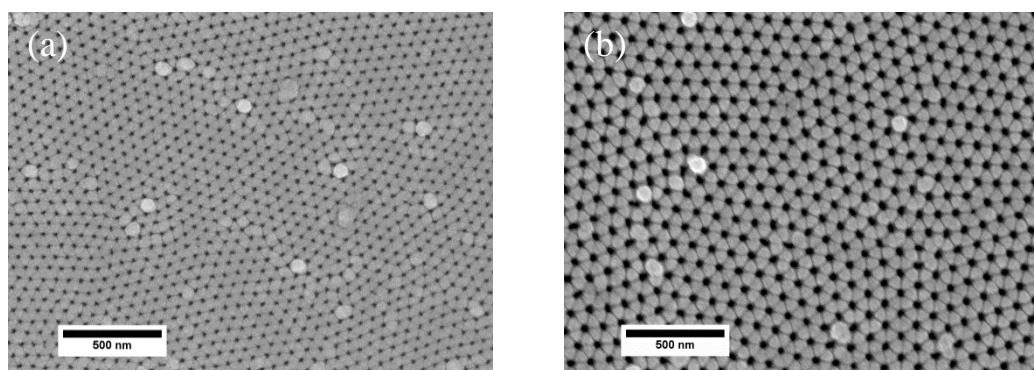


Figure 1. SEM top view of AAO fabricated in a) sulfuric acid (0.3M, 25V) and b) oxalic acid (0.3M, 40V)

In contrast to sulfuric acid, oxalic acid is non-corrosive, much more benign to handle. More importantly, AAO formed in oxalic acid results in larger pore size and higher degree of order. Usually AAO film with larger pore size is better for template applications, since synthesized materials can fill into the large pores easily. Thus we choose oxalic acid for further studies.

Growth rate in different concentrations

The growth rate of AAO obtained in different anodizing conditions is estimated by the thickness of AAO layers divided by anodizing time, and the results are plotted in Figure 2 below. For a given anodizing voltage, higher current density can be observed in more concentrated oxalic acid solution, resulting in faster growth rate. It is well agreed with Faraday's law that the current density has a linear relationship with mole of aluminum consumed (thickness of AAO layer) in anodizing process. According to the high field conduction theory (11), current density is exponentially proportional to the applying potential. The growth rate of AAO film in Figure 2 is consistent with such theory and shows the exponential increase in higher anodizing voltage.

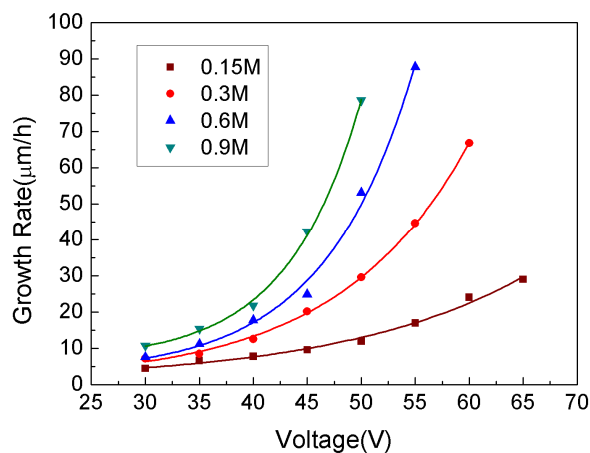


Figure 2. Growth rate of AAO with different anodizing voltages and electrolyte concentrations

Although higher growth rate of AAO can be obtained in more concentrated electrolyte, anodization should be carefully performed to avoid burning. When anodizing voltage exceeds the upper limit value, burning often happens due to large heat generated at high current density. As shown in Figure 3, the current-time curve is recorded in 0.9M oxalic acid under different anodizing voltages. Anodizing current under 55V shows strong oscillation and eventually causes burning. Table I compares the upper limit anodizing voltages, the corresponding growth rates and current densities under limit voltage in different oxalic acid concentrations. Due to the limitation of programmable power supply we used in this study, anodization voltage could only rise 5 volt in a step. Thus the limit voltage is defined as the voltage next to the burning one. As we can see, upper limit voltage decreases with the rise of electrolyte. Note that the limit anodizing voltage could decrease with the increase of electrolyte concentration, and the pore size commonly has a linear relationship with anodization voltage. Therefore, large pore size could be obtained with the combination of low electrolyte concentration and high anodizing voltage. Under our current experiment condition, AAO film forms in 0.6M oxalic acid is optimal, resulting in fast growth rate without burning and regular pore arrangement.

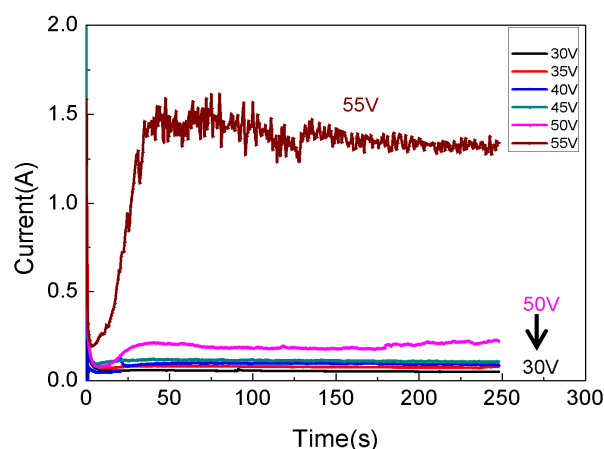


Figure 3. Current density recorded in 0.9M oxalic acid under different anodizing voltages, current showed strong oscillation when anodizing voltage rised to 55V.

TABLE I. Limit anodizing voltage for various oxalic acid concentrations

Oxalic acid concentration (M)	Limit anodizing voltage (V)	Limit growth rate ($\mu\text{m}/\text{h}$)	Current density under limit voltage (mA/cm^2)
0.15	65	29.0	18.3
0.3	60	68.5	37.6
0.6	55	87.8	48.3
0.9	50	78.6	43.1

Morphology feature of AAO

The characteristic parameters of AAO template include pore size, inter pore distance, and porosity, which varies with different anodizing conditions. Data are estimated by statistic values obtained by SEM top views and are presented in Figure 4.

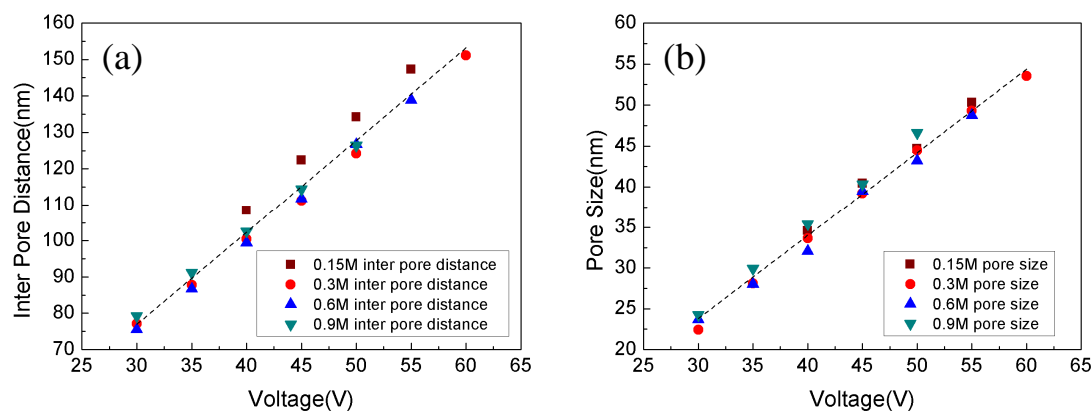


Figure 4. Influence of electrolyte concentration and anodizing voltage on **a)** pore size and **b)** inter pore distance of AAO specimen

As shown in Figure 4, both pore size (D_p) and inter pore distance (D_c) show a linear relationship with anodizing voltage as follows:

$$D_p = \xi_1 * U + b_1 \quad [1]$$

$$D_c = \xi_2 * U + b_2 \quad [2]$$

Deduced from Figure 4 the proportional factor ξ_1 and ξ_2 is about 1.05nm/V and 2.5nm/V, respectively. They are consistent with values reported in literature (2). At the same time, for a given anodizing voltage, oxalic acid concentration has nearly no effect on distribution of the pore size and inter pore distance. AAO prepared in 0.15M probably has slightly larger inter pore distance than others. In another word, electrolyte concentration has no impact on the morphology but is an effective parameter to adjust anodization rate.

Study on the branched growth of AAO

The above study shows high concentration of oxalic acid promotes the AAO growth rate without affecting its morphology. These are quite important when forming branched structures, since the competitive growth often happens in the branched growth process (12) and high growth rate may enhance the competitive mechanism. Commonly lowering the anodizing voltage leads to the branched growth of AAO and the number of newly grown branches follow the $1/\sqrt{n}$ rule (13).

Typical current-time transient when lowering anodizing voltage is shown in Figure 5(a). Initially, current is minimal due to thicker barrier layer formed during last high anodizing voltage step. Then, the barrier layer gets thinned down gradually under electric field, leading to the increase of current and this is the stage of branches formation. After a while, the thickness of barrier layer reaches the critical value and keeps constant under the effect of electric field (14). New balance achieves with the steady growth of nano channels.

Samples were made in a series of concentration (0.3M, 0.4M, 0.5M, 0.6M, and 0.9M, respectively) with the voltage dropped from 50V to 35V to form one to two channels. Results in Figure 5(b) indicate high electrolyte concentration can promote

current density and shorten the time for barrier thinning process. This could be due to high electric conductance in relatively high oxalic acid concentration. On one hand the electric conductance increases with the increase of electrolyte concentration for lower concentration. On the other hand, the effect is saturated when the electrolyte concentration exceeds the limit value (0.6M). The reason might be that oxalic acid is a weak electrolyte, so the dissociation of hydrogen ion has reached a balance in a relative high concentration.

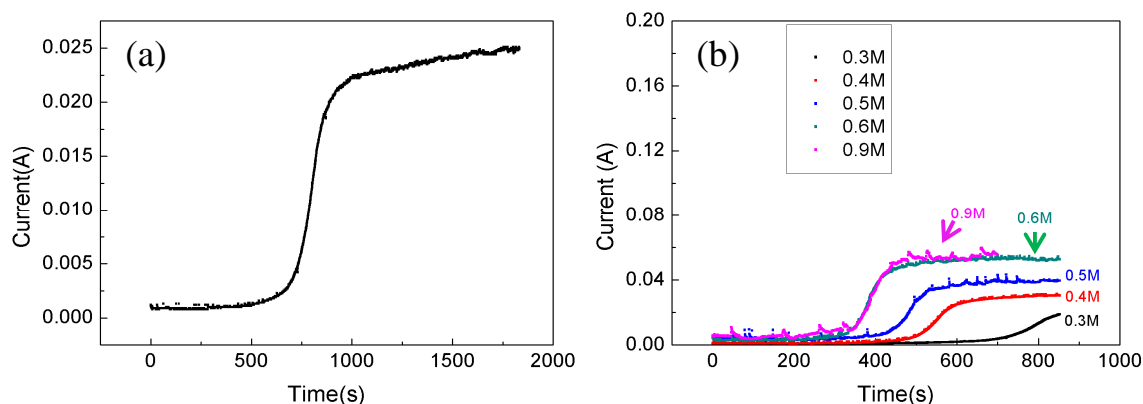


Figure 5. **a)** The current-time transient for typical branch growth when voltage drops from 50V to 35V, **b)** Current-time transient during the process of voltage lowering in different electrolyte concentrations.

By applying cyclic high-low voltage (50V-30V) and anodizing in 0.6M oxalic acid the “fish-bone” like AAO template is fabricated as shown in Figure 6. The relatively high oxalic acid concentration is the major factor for promoting the competitive growth. As the competitive degree can be controlled by the electrolyte concentrations, while the channel diameters keep unchanged to grow desired nano-structures.

The reason we call it “fish-bone” like is because it contains a main channel with several side branches. When the nearby two branches touch, they stop growing and new branches grow at the end of the etch front. Balance reaches after tens of minutes and all channels at the end of the branch grow vertical to the film. The entire branching process for one cycle can last for a while that the length of each branched channel layer is about 1~2 micrometers, after that voltage needs to be increased to 50V again. We believe that the “fish-bone” like AAO may be one kind of promising template that the main channels in “fish-bone” structure provide direct through way for chemicals. When used as template to fabricate porous carbons, the synthesized structure will have direct electron pathway with large surface area resulting from such structure, which may provide high electron transport for various applications.

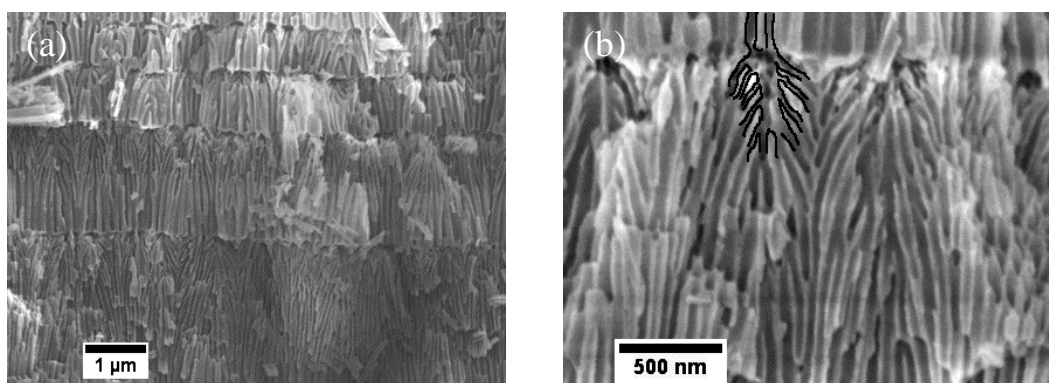


Figure 6. **a)** Cross sectional SEM images of multilayer fish-bone like AAO nanochannels, **b)** zoom of a complete “fish-bone”.

More interestingly, the “fish-bone” structure demonstrates a superior hydrophilic property. Figure 7 compares two 55 μm -thickness AAO samples while “fish-bone” like nanochannel presents a much lower water contact angle. The average water contact angle is about 60° for the straight channel AAO (Figure 7(a)) while the related value is about 15° for “fish-bone” like AAO (Figure 7(b)). Moreover, water drops spread out on the fish-bone like channels very quickly. Strong wettability of the branched nano channels may due to high porosity and large specific area of AAO template which can improve pore filtration for template synthesis.

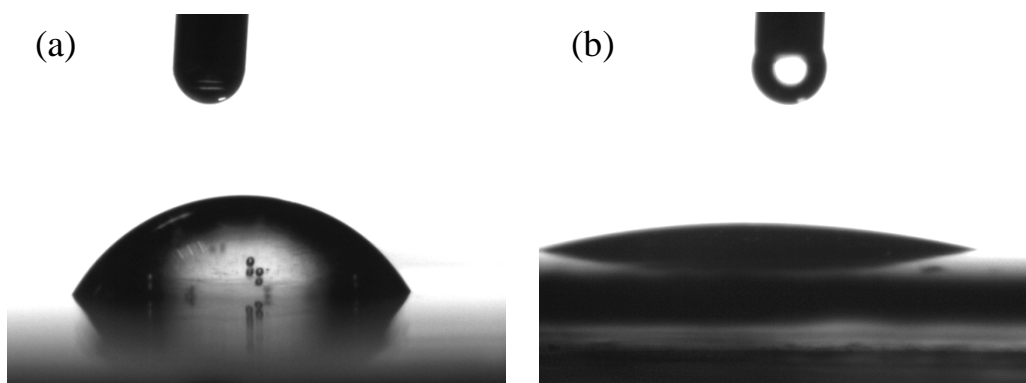


Figure 7. Snapshots of water contact angle on: **a)** conventional AAO fabricated in 0.6M 50V ($60^\circ \pm 1^\circ$), **b)** fish-bone like AAO film ($15^\circ \pm 1^\circ$ initially and the water drop quickly spreads into AAO film)

Conclusions

In this paper, structural features of AAO prepared in different oxalic acid concentration and anodizing voltage have been discussed. Higher electrolyte concentration results in faster growth rate of AAO films while has little influence on the pore size and inter pore distance. High electrolyte concentration can also promote the branched growth. By optimizing experimental condition, fish-bone like AAO nanochannels is fabricated and demonstrates superior hydrophilic property. This would lead to further synthesis work by such template.

Acknowledgements

The authors want to thank Wenjuan Yang for SEM support and Xiang Li for some discussion. We also would like to acknowledge AMETEK lab for equipment and technical supports. This work is supported by NSFC (51101064), National Key Basic Research Program of China (2013CB934800), the Fundamental Research Funds for the Central Universities, HUST (2012TS076), Thousand Young Talents Plan, the Recruitment Program of Global Experts and State Key Laboratory of Digital Manufacturing Equipment and Technology Funding (0225100053).

Reference

1. A. B. F. Martinson, J. W. Elam, J. T. Hupp and M. J. Pellin, *Nano Lett.*, **7**, 2183 (2007).
2. G. D. Sulka and W. J. Stepniowski, *Electrochim. Acta*, **54**, 3683 (2009).
3. G. Meng, Y. J. Jung, A. Cao, R. Vajtai and P. M. Ajayan, *Proc. Natl. Acad. Sci. USA*, **102**, 7074 (2005).
4. A. Y. Y. Ho, H. Gao, Y. C. Lam and I. Rodríguez, *Adv. Funct. Mater.*, **18**, 2057 (2008).
5. D.-L. Guo, L.-X. Fan, F.-H. Wang, S.-Y. Huang and X.-W. Zou, *J. Phys. Chem. C*, **112**, 17952 (2008).
6. S. Jeon, V. Malyarchuk, J. O. White and J. A. Rogers, *Nano Lett.*, **5**, 1351 (2005).
7. J. Li, C. Papadopoulos and J. Xu, *Nature*, **402**, 253 (1999).
8. B. Chen, Q. Xu, X. Zhao, X. Zhu, M. Kong and G. Meng, *Adv. Funct. Mater.*, **20**, 3791 (2010).
9. A. P. Li, F. Müller, A. Birner, K. Nielsch and U. Gösele, *J. Appl. Phys.*, **84**, 6023 (1998).
10. F. Li, L. Zhang and R. M. Metzger, *Chem. Mater.*, **10**, 2470 (1998).
11. W. Lee, R. Ji, U. Gosele and K. Nielsch, *Nat. Mater.*, **5**, 741 (2006).
12. C. Shuoshuo, L. Zhiyuan, H. Xing, Y. Hui and L. Yi, *J. Mater. Chem.*, **20**, 1794 (2010).
13. C. Shuoshuo, L. Zhiyuan, H. Xing and L. Yi, *J. Mater. Chem.*, **19**, 5717 (2009).
14. Z. Su, G. Hähner and W. Zhou, *J. Mater. Chem.*, **18**, 5787 (2008).